JACS ARTICLES

Published on Web 01/22/2009

$Ru(bpy)_3$ Covalently Doped Silica Nanoparticles as Multicenter Tunable Structures for Electrochemiluminescence Amplification

Simone Zanarini,*,† Enrico Rampazzo,*,† Leopoldo Della Ciana,‡ Massimo Marcaccio,† Ettore Marzocchi,‡ Marco Montalti,† Francesco Paolucci,*,† and Luca Prodi*,†

Dipartimento di Chimica "G. Ciamician", Universitá di Bologna, Via Selmi 2, 40126 Bologna, Italy and Cyanagen srl via Stradelli Guelfi, 40/c, 40138 Bologna, Italy

Received September 30, 2008; E-mail: simone.zanarini@unibo.it; enrico.rampazzo@unibo.it

Abstract: The electrochemiluminescence (ECL) of doped silica nanoparticles (DSNPs), prepared by a reverse microemulsion method that leads to covalent incorporation of the $Ru(bpy)_3^{2+}$, was investigated in acetonitrile and aqueous buffers. The emission was produced for the first time by cation−anion direct annihilation, and the position of ECL maxima indirectly allowed estimation of the $E_{1/2,IOx}$ and $E_{1/2,IRed}$ potentials for $Ru(bpy)_3$ inside DSNPs. The weak ECL emission is most likely generated by an intrananoparticle ruthenium unit annihilation rather than by the electron transfer between a reduced and oxidized DSNP due to the very low diffusivities of the nanoparticles. Thiol-terminated DSNPs were self-assembled on gold substrates, forming compact and stable monolayers which mimic probe−target assays with DSNPs as labels. The ECL intensity obtained by such functionalized substrates in aqueous media, using tripropylamine (TPrA) as coreactant, was surprisingly increased with respect to direct electrochemical oxidation because of the ability of oxidized TPrA to diffuse within the DSNPs structure and reach a higher number of emitting units with respect to direct electron tunneling. The experimental results have been explained by proposing a basic physical−chemical model which supports evaluation of the number of redox-active centers per nanoparticle. In the model the contrasting effects of increased luminescence quantum yield and decreased diffusion coefficient with respect to free (i.e., not bound within the silica structure) emitting molecules were taken into account. This allows, in principle, optimizing the ECL emission intensity as a function of DSNP size, doping material, charge, doping level, supporting electrolyte, electrode material, and solvent. Finally, it is worth noting that this study has provided a more than 1000-fold increase of the ECL signal of a chemically and electrochemically stable DSNP compared to that of a *single dye*, suggesting that use of this kind of nanostructures as luminescent labels represents a very promising system for ultrasensitive bioanalysis.

Introduction

Preparation of silica nanoparticles internally doped with organic and inorganic fluorophores and their use as labels to improve luminescence detection limit of biomolecules was a widely investigated and effective approach.[1] The nanoparticle (NP) silica array or alternatively extended dendrimeric structures[2] allows, in fact, encapsulating a large amount of emitting molecules in a single target binding site and at the same time to partially screen the doping material from oxygen and water quenching; another advantageous feature is the fixed position of the molecules inside NP-limiting self-quenching phenomena.[3] Lately, electrogenerated chemiluminescence (ECL) from $Ru(bpy)_3$-doped silica nanoparticles, in solution and incorporated into nano- and microstructures, has been reported in the presence of tripropylamine (TPrA).[4] Leakage of doping material appeared however to be severely preventing a clear interpretation of the ECL experiments. Starting from the successful preparation of

† Universita di Bologna.

‡ Cyanagen srl via Stradelli Guelfi.

(1) (a) Zhao, X.; Tapec-Dytioco, R.; Tan, W. *J. Am. Chem. Soc.* **2003**, *125* (38), 11474. (b) Santra, S. M.; Zhang, P.; Wang, K.; Tapec, R.; Tan, W. *Anal. Chem.* **2001**, *73*, 4988. (c) For an overview in classical detection methods based on luminescence and chemiluminescence, see: Van Dyke, K.; Van Dyke, C.; Woodfork, K. *Luminescence biotechnology: Instruments and applications*; CRC Press: Boca Raton, 2002.

(2) Staffilani, M.; Hoss, E.; Giesen, U.; Schneider, E.; Hartl, F.; Josel, H.-P.; De Cola, L. *Inorg. Chem.* **2003**, *42* (24), 7789.

(3) (a) Wang, L.; Yang, C.; Tan, W. *Nano Lett.* **2005**, *5* (1), 37. (b) Montalti, M.; Prodi, L.; Zacheroni, N.; Zattoni, A.; Reschiglian, P.; Falini, G. *Langmuir* **2004**, *20*, 2989–2991. (c) Montalti, M.; Prodi, L.; Zaccheroni, N.; Battistini, G.; Marcuz, S.; Mancin, F.; Rampazzo, E.; Tonellato, U. *Langmuir* **2006**, *22* (13), 5877–5881. (d) Rampazzo, E.; Bonacchi, S.; Montalti, M.; Prodi, L.; Zaccheroni, N. *J. Am. Chem. Soc.* **2007**, *129*, 14251–14256. (e) Prodi, L. *New J. Chem.* **2005**, *29*, 20–31.

(4) (a) Zhang, L.; Dong, S. *Anal. Chem.* **2006**, *78* (14), 5119. (b) Zhang, L.; Dong, S. *Electrochem. Commun.* **2006**, *8*, 1687. (c) Qian, L.; Yang, X.-R. *Adv. Funct. Mater.* **2007**, *17* (8), 1353. (d) Wei, H.; Wang, E. *Chem. Lett.* **2007**, *36* (2), 210. (e) Guo, S.; Wang, E. *Electrochem. Commun.* **2007**, *9*, 1252. (f) Zhang, L.; Liu, B.; Dong, S. *J. Phys. Chem. B* **2007**, *111*, 10448. (g) Wei, H.; Zhou, L.; Li, J.; Liu, J.; Wang, E. *J. Colloid Interface Sci.* **2008**, *321*, 310. (h) Hui, W.; Jifeng, L.; Lingling, Z.; Jing, L.; Xiue, J.; Jianzhen, K.; Xiurong, Y.; Shaojun, D.; Erkang, W. *Chem.-Eur. J.* **2008**, *14* (12), 3687. (i) Hun, X.; Zhang, Z. *Sens. Actuators B* **2008**, *131*, 403.

 10.1021/ja8077158 CCC: $40.75

Scheme 1

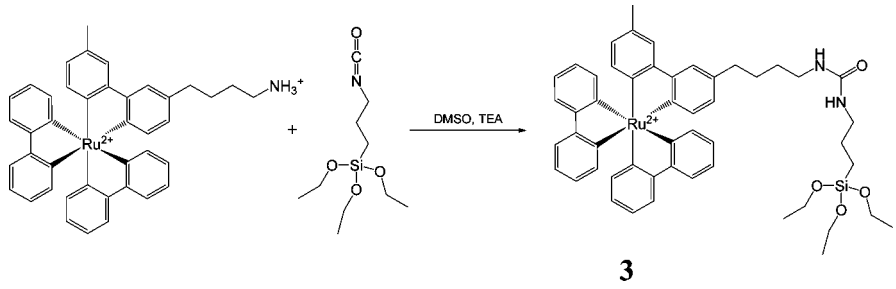

3

$Ru(bpy)_3^{2+}$ covalently doped silica nanoparticles (DSNPs), similarly reported by the Wang group in a very recent paper,[5] by taking advantage of the stability of the doping, the present contribution is an attempt to provide insight into the effects of nanoparticle incorporation in the electrochemical and ECL behavior of the doping material. The approach presented here is a combination of electrochemical, photophysical, and ECL experiments with a basic model to correlate the DSNP behavior with their tunable chemical−physical properties. ECL studies were performed first in acetonitrile (MeCN) solution where the potential of the first oxidation and reduction of doping material was estimated from the position of ECL emission peaks. Surprisingly, the relatively weak ECL emission appeared to be generated by electron transfer between oxidized and reduced $Ru(bpy)_3$ units placed in close regions within the same nanoparticle. Successively, DSNPs carrying thiol groups (DSNP-SH) were deposited as self-assembled layers on gold substrates and investigated in aqueous media. Their preparation, first reported here, was a route to suppress the negative effect of DSNP slow diffusion to the electrode affecting the electrochemical generation of radical cation and thus the ECL intensity. Under these conditions the key role played by diffusion of oxidized tripropylamine (TPrA) was evidenced, for the first time, which increases the effective number of $Ru(bpy)_3$ emitting units per NP. As final step, a simple chemical−physical model was built to support the experimental evaluation of the number of $Ru(bpy)_3$ molecules per DSNP that can be effectively considered as redox centers in ECL generation. This value was obtained by comparing the ECL intensity of the free doping molecule with that of DSNP from solutions having the same absorbance. The model developed and the simple measurements necessary can be useful in the optimization of ECL performance by varying DSNP size, charge, doping material, doping level, ECL coreactant, supporting electrolyte, electrode material, and solvent.

The interesting perspective of this study, which shows an estimated ECL intensity increase of 3 orders of magnitude from a single dye to DSNP, is the use of this kind of nanostructures in ultrasensitive bioanalysis, possibly preventing or limiting the use of amplification methods as polymerase chain reaction.

Experimental Section

Materials. All reagents and solvents were used as received without further purification. Igepal CO-520 (polyoxoethylene nonyl phenol ether), tetraethyl ortosilicate (TEOS, 99.99%), ammonium hydroxyde solution (NH_3 28−30 wt % in water), and the dye tris(2,2′-bipyridyl)dichlororuthenium(II) ($Ru(II)(bpy)_3Cl_2 \cdot 6H_2O$), **1**, were purchased from Aldrich. Reagent-grade cyclohexane, 3-isocyanatopropyltriethoxysilane, 3-mercaptopropyltriethoxysilane, and triethylamine were purchased from Fluka. The $Ru(bpy)_3^{2+}$ amine derivative, bis(2,2′-bipyridine)-[4-(4′-methyl-2,2′-bipyridin-4-yl)aminobutyl]ruthenium(II) bis(hexafluorophosphate), **2**, was supplied by Cyanagen srl (Bologna, Italy).

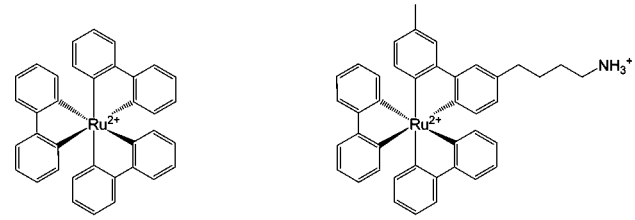

1 **2**

Water used in the described procedures was obtained from a Milli-Q Millipore water purification system and had a measured resistivity of 18 MΩ.

Synthesis of Ru(II) Derivative 3. This compound was obtained as the coupling adduct of bis(2,2′-bipyridine)-[4-(4′-methyl-2,2′-bipyridin-4-yl)aminobutyl]ruthenium(II) bis(hexafluorophosphate), **2**, and 3-isocyanatopropyltriethoxysilane (Scheme 1).

A DMSO solution of 3-isocyanatopropyltriethoxysilane (100 μL, 20 mM) and triethylamine (0.25 μL, 0.0018mmol) was added to **2** (1.6 mg, 0.0017 mmol). The reaction mixture was kept stirring at room temperature for 20 h. The presence of adduct **3** was verified by HPLC ESI-MS, and the reaction mixture was directly put to use in the nanoparticles synthesis.

ESI-MS (CH_3CN): *m*/*z* (M/2 + CH_3CN) 470 − 471 − 472.

Nanoparticles Synthesis. Dye-doped silica nanoparticles containing derivative **3** (DSNP) were synthesized at room temperature (25 °C) with a ternary microemulsion system composed of the nonionic surfactant Igepal CO-520, cyclohexane, and water.[6] For the nanoparticles synthesis, 1.92 g of Igepal CO-520, 5.00 mL of cyclohexane, 333 μL of water, and 12 μL of ammonia (28−30 w % in water) were added in a 20 mL glass vial under rapid magnetic stirring. After a 20 min equilibration time 100 μL of the reaction mixture containing the Ru(II) triethoxysilane derivative **3** was added to the microemulsion; after another 10 min 82 μL of a TEOS solution in cyclohexane (1/1 v/v) was added.

The microemulsion system was stirred for an additional 24 h prior to use for successive nanoparticle surface modification steps.

Preparation of DSNP-SH. Passivation of the DSNP surface was obtained using 3-mercaptopropyltriethoxysilane as the source of thiol groups. A solution of 3-mercaptopropyltriethoxysilane in cyclohexane (24 mM, 20 μL) was added to a small amount of DSNP microemulsion (50 μL) housed in a 1.5 mL plastic vial, and this

(5) Li, M.; Chen, Z.; Yam, V. W.; Zu, Y. *ACS Nano* **2008**, *2* (5), 905.

(6) For basics around NP synthesis, structure, and properties, see:(a) Cushing, B. L.; Kolesnichenko, V. L.; O'Connor, C. J *Chem. Rev.* **2004**, *104*, 3893. (b) Liveri, T. V. *Controlled Synthesis of Nanoparticles in Microheterogeneous Systems*; Springer:New York, 2006. (c) Schmid, G., Ed. *Nanoparticles from theory to application*; Wiley-VCH: Weinheim, 2004. (d) Schwarz, J. A., Contescu, C. I., Eds. *Surfaces of nanoparticles and porous materials*; Marcel Dekker: New York, 1999. (e) Feldheim, D. L.; Foss, C. A. *Metal nanoparticles: Synthesis, characterization and applications*; Marcel Dekker: New York, 2002.

mixture was stirred for 24 h at room temperature. After this time the microemulsion system was directly used for DSNP-SH deposition on gold electrodes.

Preparation of the Self-Assembled Layers of DSNP-SH on Gold Electrodes. Silicon chips with sputtered gold electrodes were supplied by Olivetti, vide infra. The chips were cleaned with freshly prepared Piranha solution at room temperature for 10 min. (Caution: Piranha solution H_2SO_4 (98%)/H_2O_2(30%) = 4/1 is an extremely strong oxidant and must be handled with care.) Each chip was then extensively rinsed with Milli-Q water and dried under vacuum. A small amount of microemulsion containing DSNP-SH (10 μL) was dropped on each chip electrode and covered with a clean microscope slide cover glass (20 × 20 mm). Chips with this setup were leaned on a flat surface and introduced in a glass desiccator. After 20 h, cover glasses were gently removed, dipping every silicon chip in ethanol. The chips were then rinsed with ethanol, Milli-Q water, and ethanol and finally dried at room temperature.

TEM Experiments. A Philips CM 100 transmission electron microscope operating at 80 kV was used. For TEM investigations a holey carbon foil supported on a conventional copper microgrids was dried under vacuum after deposition of a drop of nanoparticles solution in EtOH.

Photophysical Measurements. UV−vis absorption spectra were performed at 25 °C by means of a Perkin-Elmer Lambda 45 spectrophotometer. The luminescence spectra were recorded with an Edinburgh FLS920 equipped with a Hamamatsu R928P photomultiplier. Quartz cuvettes with an optical path length of 1 cm were used.

Particles Size Distribution. Dynamic light scattering (DLS) was used for determination of the silica nanoparticles size distributions employing a Malvern Nano ZS instrument with a 633 nm laser diode. Samples were housed in quartz cuvettes of 1 cm optical path length. The width of the DLS hydrodynamic diameter distribuition is indicated by the PdI (polydispersion index). In the case of a monomodal distribuition (Gaussian) calculated by means of cumulant analysis PdI = $(\sigma/Z_{avg})^2$, where σ is the width of the distribuition and Z_{avg} is average diameter of the particles population.

Electrochemistry and Electrochemiluminescence (ECL). Electrochemical and ECL experiments were performed either in aqueous phosphate buffer solutions (PB) containing equimolar (0.1 M) quantities of Na_2HPO_4 and KH_2PO_4 (from Sigma-Aldrich) at pH 7.5 or in MeCN (absolute over molecular sieves from Aldrich) and 0.1 M tetrabutylammonium hexafluorophosphate ($TBAPF_6$, from Sigma-Aldrich) solutions. In all experiments except those where ECL was obtained by direct cation−anion annihilation. Tripropylamine (TPrA) was added as an oxidative coreactant at a concentration of 3×10^{-2} M (maximum concentration at this pH). ECL was generated by a single oxidative step including both the TPrA and Ru complex oxidations according to well-established methods.[7] An AUTOLAB potentiostat (Ecochemie, Holland) was used in the electrochemical experiments, while the ECL signal was measured with a photomultiplier tube (PMT, Hamamatsu model R255) placed a few millimeters in front of the working electrode whose signal was preamplified with an ultralow noise current preamplifier (Acton research model 181) before acquisition via the second input channel of AUTOLAB. The ECL spectrum was recorded by inserting the same PMT in a dual-exit monochromator (ACTON RESEARCH model spectra pro 2300i). Photocurrent detected at PMT was accumulated for 3−5 s depending on the emission intensity for each monocromator step. PMT was biased at 750 V, except when differently specified.

Three different types of working electrodes were used in the experiments: (i) Glassy carbon disk electrodes (GC, diameter 3 mm); (ii) gold disk electrodes (diameter = 2 mm) sputtered onto silicon (with a Ti/Ta underlayer) previously described[8] were used to prepare DSNPs self-assembled monolayers; (iii) Commercial disk screen-printed electrodes (SPE, DROPSENS, model DS220 AT), comprising a 4 mm gold working electrode, a carbon ring counter electrode, and a quasi-reference Ag wire. These electrodes were used for quantitative and repeated measurements in view of the low volume of solution needed (20−40 μL/sample) and the high reproducibility of surface properties. The SPEs were contacted with a USB-like interface (DROPSENS model DSC system) and the PMT was carefully positioned in front of the working electrode to improve ECL signal reproducibility. Either an Ag wire quasi-reference electrode or an Ag/AgCl electrode was used as the reference electrode. The quasi-reference Ag electrode was polished with 0.05 μm alumina, sonicated, and thoroughly rinsed with Milli-Q water and acetone before each run. When the silver electrode was used the potential values referred to SCE (saturated calomel electrode) have been calculated by adding ferrocene as an internal standard. A platinum spiral was used as the counter electrode with a type (i) working electrode.

Results and Discussion

Dynamic Light Scattering Measurements. Evaluation of nanoparticles size has been obtained through transmission electron microscopy (TEM) and dynamic light scattering (DLS) measurements. A TEM image of DSNP is shown in Figure S1, Supporting Information. A pretty homogeneous size around 18 nm can be noted. A quantitative size evaluation in solution has been obtained with DLS. (The DSNP size distribution diagram is shown in Figure S2, Supporting Information.) In ethanol (η_{EtOH} = 1.0740 cP, n = 1.3610, T = 25 °C) the medium hydrodinamic DSNP diameter (d_{NP}) has been found to be 32 nm (PdI = 0.103).

Cyclic Voltammetry and Electrochemically Generated Luminescence of DSNPs in Solution. Cyclic voltammetric investigation of a 10^{-5} M DSNPs MeCN/$TBAPF_6$ solution was carried out under similar conditions to those previously described.[9] The cyclic voltammetric curves, as shown in Figure 1a, displayed a mainly capacitive-like behavior that in the negative potential region was barely distinguishable from the background curve. On the other hand, in the positive potential region (Figure 1) an anticipated irreversible discharge was observed (by about 1 V with respect to the MeCN/$TBAPF_6$ baseline) associated to the unavoidable water contamination from the DSNPs sample (see above). The absence of diffusion-like voltammetric signals clearly associated to redox processes involving the Ru complex in the DSNPs is ascribed to the very low diffusion coefficient expected for the nanoparticles (vide infra) as well as to the relatively low concentration of redox-active complexes within the DSNPs.[10] Interestingly, following the irreversible process at ca. +1.4 V the CV curves also display an irreversible cathodic peak located at ca. −1.5 V (process 1, Figure 1a). The intensity of such a peak does not build up upon repetitive cycling, thus excluding that such a peak is associated to the irreversible release of the Ru complex from the DSNPs. It would rather correspond to the discharge of entrapped (positive) charges accumulating during the DSNP oxidation; a similar behavior has often been

(7) (a) Bard, A. J., Ed. *Electrogenerated chemiluminescence*; Marcel Dekker: New York, 2004. (b) Richter, M. M. *Chem. Rev.* **2004**, *104*, 3003. (c) Miao, W. *Chem. Rev.* **2008**, *108*, 2506.

(8) Zanarini, S.; Rampazzo, E.; Bich, D.; Canteri, R.; Della Ciana, L.; Marcaccio, M.; Marzocchi, E.; Montalti, M.; Panciatichi, C.; Pederzolli, C.; Paolucci, F.; Prodi, L.; Vanzetti, L. *J. Phys. Chem. C.* **2008**, *112* (8), 2949.

(9) Zanarini, S.; Bard, A. J.; Marcaccio, M.; Palazzi, A.; Paolucci, F.; Stagni, S. *J. Phys. Chem. B* **2006**, *110* (45), 22551.

(10) This hypothesis is supported by the results discussed in the following ECL section showing that the potential of the first reductive process of DSNP is practically identical to that of free $Ru(bpy)_3^{2+}$.

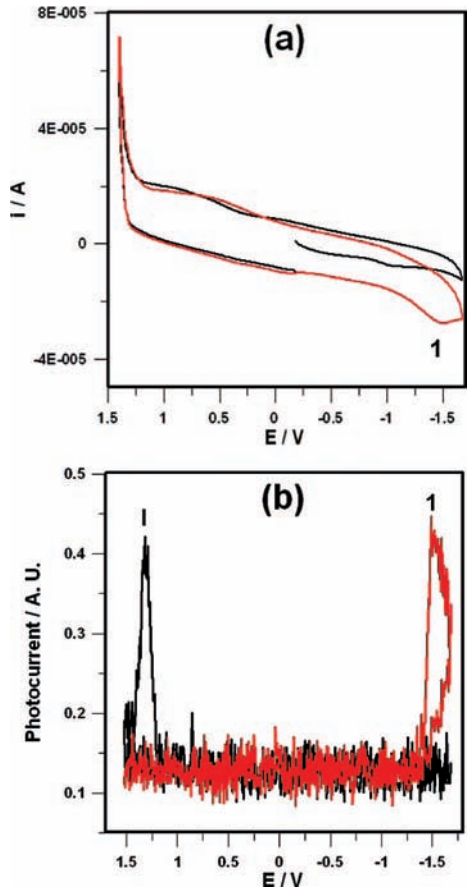

Figure 1. Typical current to potential (a) and light to potential (b) synchronized curves of Ru(bpy)$_3$ DSNP collected during the first (black line) and third (red line) voltammetric cycle. Working electrode was a 3 mm GC disk, and a Pt wire was used as the counter electrode. The curves were obtained from a 10^{-5} M Ru solution in MeCN /TBAPF$_6$ 10^{-1} M. The sample was Ar degassed for ca. 10 min. Scan rate: 1 V/s, and potential range $E_0 = 0$ V, $E_1 = -1.5$ V, $E_2 = 1.7$ V. Potentials are referred to SCE.

described in the CV investigation of conducting and redox polymers.[11] The presence of entrapped charges following oxidation of DSNPs would in fact explain the observed asymmetry in ECL generation between the oxidative and reductive routes, as described below.

In spite of the absence of any clear evidence of redox activity in the Ru complexes in the DSNPs fairly intense ECL was generated from the above DSNP solutions under voltammetric and chronoamperometric experiments. The conditions used in such experiments suggest that ECL is generated according to an annihilation mechanism involving either oxidized or reduced Ru(bpy)$_3$ units in a similar manner to the behavior of the free complex in solution. Figure 1b shows, in fact, that ECL is detected at both negative (around -1.5 V) and positive (around 1.3 V) potentials that are compatible with the reduction and oxidation, respectively, of the complex within the DSNPs. It has, in fact, been previously shown[12] that the potentials where ECL maxima are obtained during potentiodynamic (voltammetric) generation of ECL at relatively low scan rates and in the absence of any coreactant, i.e., by the annihilation route, are good estimates of the redox potentials relative to the reduction and oxidation of the emitting species. Accordingly, the $E_{1/2,IOx}$ and $E_{1/2,I\ Red}$ of the emitting species would then correspond in this case to the values given above. In solution, the free Ru complex precursor **2** was found to reduce at -1.48 V and oxidize at $+1.31$ V vs SCE, in very good agreement with the above result.

Chronoamperometric experiments also confirmed the ability of DSNPs to promote ECL at potentials compatible with the reduction and oxidation of the Ru complexes (Figure 2a and 2b). Analysis of the light-time transients clearly indicated a much shorter lifetime for the ECL process generated at positive potentials with respect to that at the negative ones, as shown in Figure 2a and 2b. Furthermore, while during the first steps ECL was observed at both positive and negative potentials, in the successive ones only emission during the negative steps was maintained. We believe that a possible explanation for such an asymmetric ECL behavior has to be found in the (positive) charge-trapping process, also observed during the CV experiments. Such a phenomenon, possibly associated to a reduced mobility of counteranions from the supporting electrolyte (PF_6^-) within the DSNPs (vis-à-vis that of countercations), would limit the lifetime of injected negative charges (following the reduction step) and hence the efficiency of the ECL generation process in the oxidation step. Further work aimed at clarifying such a behavior is in progress, and results will be reported in due course.

Finally, in view of the low diffusion coefficient of DSNPs (~25 times lower than the free complex, vide infra) we expect that only the DSNPs located within a very thin layer close to the electrode surface may participate in generation of ECL. Furthermore, we also expect that the annihilation mechanism involves rather than the encounter of two NPs (one oxidized and one reduced) the intra-NP electron transfer between regions of (trapped) oxidized and reduced Ru(bpy)$_3$ units.

Electrochemistry and Electrochemiluminescence of DSNP Self-Assembled Monolayers on Gold. DSNP-SH self-assembled monolayers (DSNP-SH SAM) were prepared on gold electrodes as described above and used to generate ECL in aqueous media in the presence of an oxidative coreactant (TPrA). DSNP-SH SAMs can be considered as model systems for probe−target assays (DNA, proteins, etc.) using the DSNP as a light emitting reporter. Our experiments showed that TPrA plays an important role in ECL signal amplification, likely thanks to TPrA diffusion into nanopores that makes a larger number of Ru(bpy)$_3$ units excited with respect to intra- or inter-NPs electron hopping.

Prior to ECL characterization the gold electrodes functionalized with DSNP-SH SAM were characterized by CV in aqueous solution containing $LiClO_4$ as supporting electrolyte. Typical CV profiles are shown in Figure S3, Supporting Information. Oxidation of Ru(bpy)$_3$ units was still not visible; in fact, the voltammetric pattern was essentially governed by two different phenomena: stripping of the DSNP-SH SAM and formation and reduction of Au oxides on the substrate. The irreversible peak observed at around $+1.1$ V during the first cycle (marked I in Figure S3a, Supporting Information) is confidently attributed to the SAM detachment during electrolysis. In the subsequent cycles a largely less intense peak is observed at relatively lower potentials ($+0.95$ V circa). Such a peak and the cathodic peak at ~0.4 V in the reverse scan (marked 1) were instead attributed to formation and subsequent reduction of an Au oxide layer whose potential is influenced

(11) (a) Heinze, J. *Encyclopedia of Electrochemistry*; Bard, A. J., Stratmann, M., Schäfer, H. J., Eds.; Wiley-VCH: Weinheim, 2004; Vol. 8, p 605. (b) Deronzier, A.; Moutet, J.-C. *Coord. Chem. Rev.* **1996**, *147*, 339.
(12) Zanarini, S.; Della Ciana, L.; Marcaccio, M.; Marzocchi, E.; Paolucci, F.; Prodi, L. *J. Phys. Chem. B.* **2008**, *112* (33), 10188.

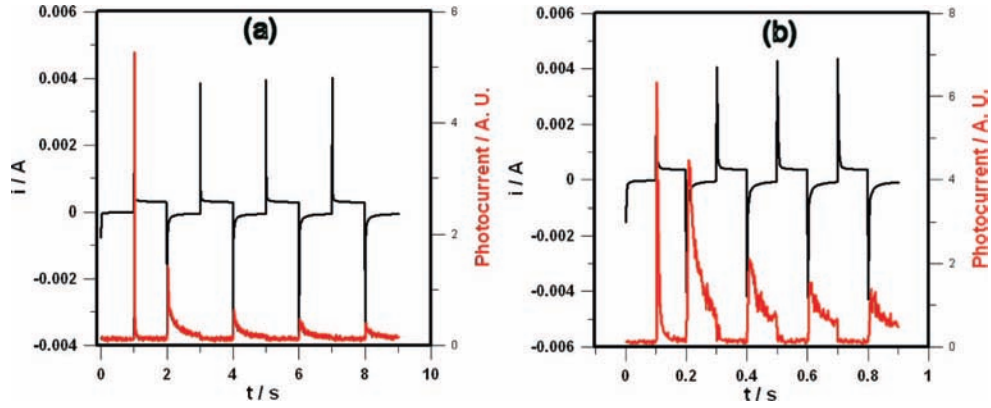

Figure 2. Light/current/time curves of $Ru(bpy)_3$ DSNP. Working electrode was a 3 mm GC disk, and a Ag wire was used as a quasi reference. The curves were obtained from a 10^{-5} M Ru solution in MeCN /$TBAPF_6$, 10^{-1} M. The sample was Ar degassed for ca. 10 min. Potential program: $E_1 = -1.5$ V s, $E_2 = 1.7$ V, (a) $t_1 = t_2 = 1$ s and sample time = 5 ms and (b) $t_1 = t_2 = 0.1$ s and sample time = 2 ms. Detection: PMT bias, 750 V; current range, 10^{-7} A/V.

by the presence of residual DSNP-SH SAM. A similar behavior is observed in Figure S3b, Supporting Information, where the reversal positive potential is progressively increased.

Electrochemiluminescence from DSNP-SH SAM in the Presence of TPrA. ECL tests were then performed by immersing freshly prepared DSNP-functionalized gold electrodes in the PB solution containing 3×10^{-2} M TPrA. Intense ECL emission was detected during the first two voltammetric scans and progressively decreased in the following ones. Because of the rapid disappearance of the ECL emission from DSNP-SH SAM a very weak spectrum was collected that was however compatible with that of $Ru(bpy)_3^{2+}$ emission (not shown). The light/current/potential profiles during the first two scans are shown in Figure 3. Unlike the previously reported case of a SAM of individual Rubpy−NH_2 (single ECL labels) investigated under similar conditions, two ECL maxima, with largely different intensities, were observed during voltammetric investigation of the present system located at +0.91 and +1.23 V, respectively, in Figure 3a and 3b. Such peaks were observed in both the first and second cycle; however, while the intensity of the peak at 1.23 V remained almost unchanged, that of the first peak decreased to about 1/10 after the first scan, thus becoming almost negligible with respect to the second one. The presence of two ECL maxima is compatible with the known mechanisms for the ECL generation in the presence of a coreactant involving either the bare electrochemical oxidation of TPrA (mechanism I in Chart 1) or that of both TPrA and $Ru(bpy)_3^{2+}$ (mechanism II in Chart 1). The dramatic change in the ECL profile can be explained on the basis of the voltammetric behavior of Au in the presence of hydrophobic coatings. It is known that use of PB as supporting electrolyte strongly limits the direct TPrA oxidation because of formation of Au oxides onto the working electrode surface (see above and Figure S3, Supporting Information). For this reason, ECL is usually generated in PB almost exclusively at the potential where $Ru(bpy)_3^{2+}$ is directly oxidized. However, the presence of the DSNP-SH SAM, analogous to the cases discussed in earlier works,[13] makes the gold surface hydrophobic and prevents formation of the Au oxide, thus increasing the amount of electrogenerated $TPrA^{\cdot+}$

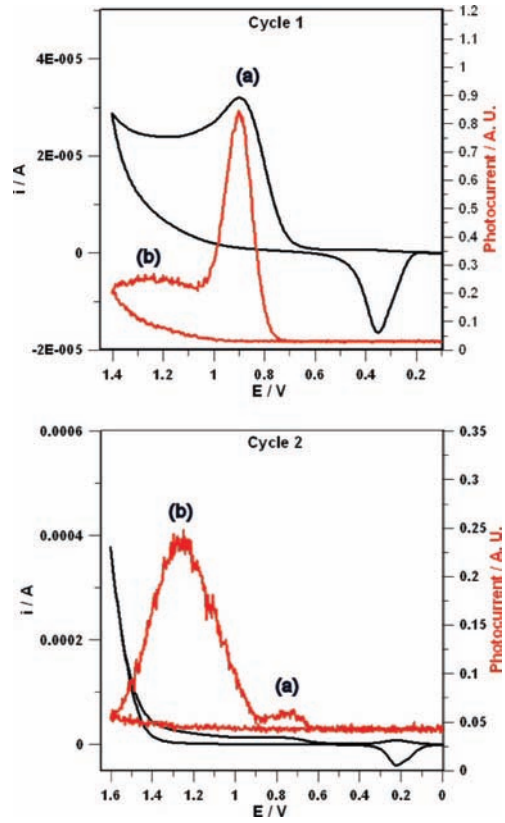

Figure 3. First and second cycle light/current/potential curve of a gold substrate functionalized with DSNP-SH self-assembled layer immersed in a 0.1 M PB (pH 7.5) containing 3×10^{-2} M TPrA. Switching method: cyclic voltammetry; scan rate, 0.5 V/s. Potentials are vs satd Ag/AgCl.

and the prevalence of mechanism I in the ECL generation (Figure 3a). In the following scans, however, after detachment of the SAM from the electrode surface (see above), such a mechanism becomes less efficient, thus explaining the observed evolution of the ECL profile.

The high intensity associated to the first maximum in the first scan highlights the important role of TPrA in promoting ECL from DSNPs: the coreactant may in fact diffuse into the silica nanopores and reach a larger number of Ru sites with respect to direct electron tunnelling (electron hopping typical distance is only ~1−2 nm from the electrode). The efficient penetration of TPrA in the silica structure has great potential for use of

(13) (a) Zu, Y.; Bard, A. *J. Anal. Chem.* **2001**, *73*, 3960. (b) Bruce, D.; McCall, J.; Richter, M. M. *Analyst* **2002**, *127*, 125. (c) Factor, B.; Muegge, B.; Workman, S.; Bolton, E.; Bos, J.; Richter, M. M. *Anal. Chem.* **2001**, *73*, 4621. (d) Workman, S.; Richter, M. M. *Anal. Chem.* **2000**, *72*, 5556.

Chart 1. Two Fundamental Mechanisms and Limiting Factors of ECL Generation in the DSNP/TPrA System

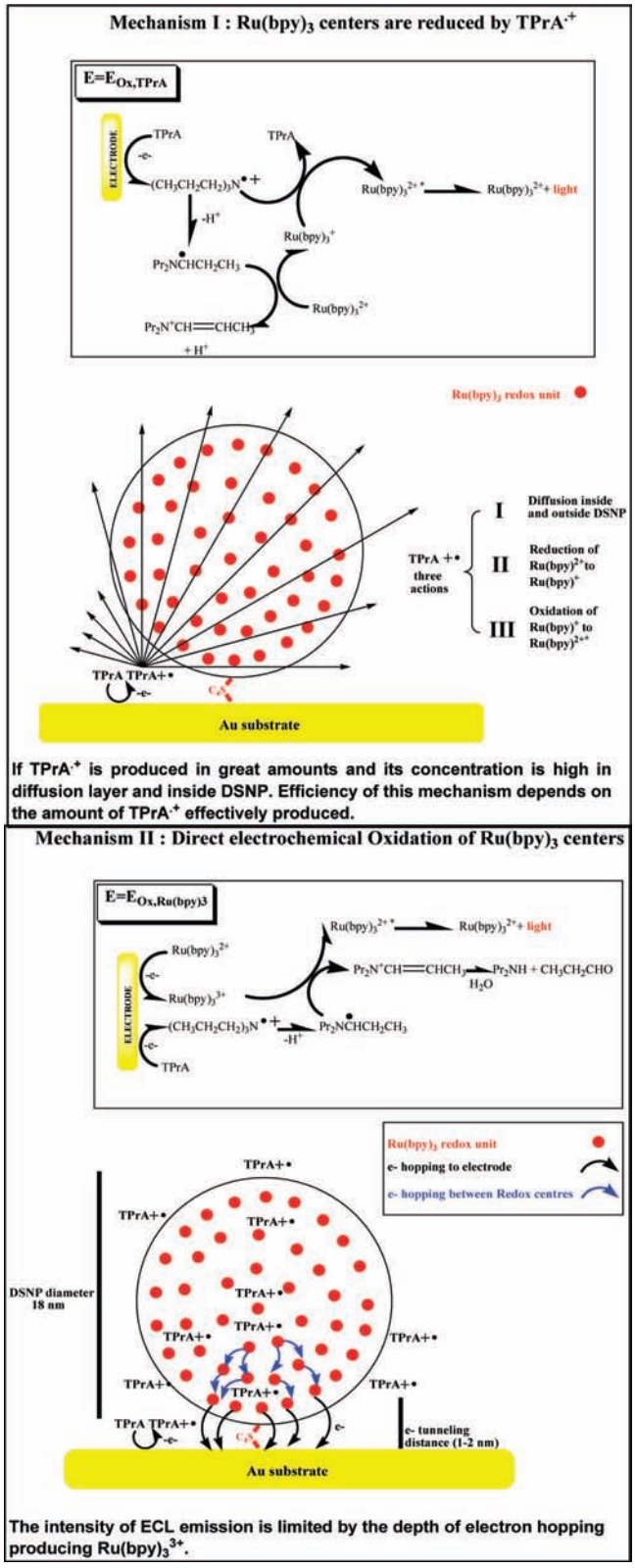

DSNP as ECL labels by significantly lowering the ECL detection limit with respect to the direct Ru oxidation mechanism. Finally, the fact that the ECL maximum intensity corresponding to the potential of direct $Ru(bpy)_3^{2+}$ oxidation (mechanism II) remains constant in the following voltammetric cycle (Figure 3b) suggests that once the hydrophobic monolayer is stripped the concentration of $Ru(bpy)_3$ units in the diffusion layer reachable by direct electron transfer from the electrode is the limiting factor for the excited-state generation, according to mechanism II (see Chart 1).

Estimating the Number of Active Redox Sites per Nanoparticle. As discussed in the previous paragraph, the ECL emission of the DSNP/TPrA system occurs according to two different prevailing mechanisms (Chart 1): depending on the concentration of electrogenerated $TPrA^{\cdot+}$, this species can act either as reducing agent of the $Ru(bpy)_3^{2+}$ centers (mechanism II) or as both reducing and oxidizing reactant (mechanism I). We now consider the ECL generation from a DSNP solution in PB and in the presence of TPrA. Without the use of surface conditioning agents such as Triton-X 100 or hydrophobic coatings of the working electrode, mechanism II, involving direct electrochemical oxidation of Ru, is normally prevailing.

Formulation of the Model. The voltammetric peak current (i_P) can be written for a Nernstian process, such as $Ru(bpy)_3^{2+}$ oxidation, as[14]

$$i_P = K\sqrt{D}c \tag{1}$$

where

$$K = (2.69\times10^5)An^{3/2}v^{1/2} \tag{2}$$

where D is the diffusion coefficient, c the molar concentration of Ru centers, A the electrode area, n the number of exchanged electrons, and v the scan rate. Considering that the ECL maximum intensity (I_{ECL}) expressed in arbitrary units is proportional to i_P (assumed here as the Faradaic current corresponding to $Ru(bpy)_3$ direct electrochemical oxidation; as discussed above, $TPrA^{\cdot+}$ is in large excess and the electrochemical production of its radical cation is not the limiting factor), we write that

$$I_{ECL} = K'\sqrt{D}c \tag{3}$$

where K' is an empirical constant depending on the specific light detection setup and includes the previously described K constant.

By dividing the maximum ECL intensity obtained from a DSNP solution ($I_{ECL,NP}$) by that of a $Ru(bpy)_3^{2+}$ reference solution ($I_{ECL,dye}$) having the same absorbance (see spectra in Figure S4, Supporting Information) and thus the same total amount, n, of $Ru(bpy)_3$ molecules it follows that

$$\frac{I_{ECL,NP}}{fI_{ECL,dye}} = \sqrt{\frac{D_{NP}}{D_{dye}}}\frac{c_{NP}m}{c_{dye}} \tag{4}$$

where m is the number of electrochemically active Ru molecules per DSNP ($m \le n$), c_{NP} the DSNP concentration, D_{NP} the nanoparticle diffusion coefficient, D_{dye} the $Ru(bpy)_3^{2+}$ diffusion coefficient, and c_{dye} the $Ru(bpy)_3$ reference solution concentration. Equation 4 is corrected by a factor f in consideration of the higher luminescence quantum efficiency of $Ru(bpy)_3$ inside DSNP ($f = \varphi_{dye,NP}/\varphi_{dye} \approx 3$).[15] The D_{NP} can be calculated from the Stokes−Einstein equation

$$D_{NP} = kT/6\pi\eta R_H \tag{5}$$

where k is the Boltzmann constant, T the absolute temperature, R_H the hydrodynamic radius, and η the medium viscosity.[16] By

(14) Bard, A. J.; Faulkner, L. R. *Electrochemical methods. Fundamentals and applications*, 2nd ed.; Wiley: New York, 2001.
(15) Found experimentally by luminescence measurements. Detailed results on the photophysics of the DSNP will be reported in a more specialized work actually in preparation.
(16) In this case the DSNP were dissolved in ethanol solution.

introducing in eq 5 the value of the mean R_H found experimentally by DLS measuments (~30 nm) we obtain that $D_{NP} = 1.1291 \times 10^{-7}$ cm^2/s, to be compared with the diffusion coefficient for the single dye, $D_{Ru(bpy)_3} = 2.710 \times 10^{-6}$ cm^2/s, obtained taking a molecular diameter of 1.5 nm for $Ru(bpy)_3^{2+}$.[17]

We consider now the two solutions displaying the spectra of Figure S4, i.e., with the same absorbance at the MLCT band maximum. This corresponds to $c_{Ru(bpy)_3} = c_{NP}n$, and by taking in account that in ethanol and with good approximation in water $\sqrt{(D_{NP})}/(D_{dye}) \approx 1/5$ from eq 4 it follows that

$$\frac{I_{ECL,NP}}{I_{ECL,dye}} = \frac{3}{5} \cdot \frac{c_{NP}m}{c_{dye}} \Rightarrow \frac{c_{NP}m}{c_{dye}} = \frac{5}{3} \cdot \frac{I_{ECL,NP}}{I_{ECL,dye}} \quad (6)$$

If we define

$$R = \frac{I_{ECL,NP}}{I_{ECL,dye}} \quad (7)$$

then R is experimentally dependent on the number of ECL active molecules within the DSNPs, $c_{NP}m$ with respect to the total c_{dye}. If all molecules inside DSNP are electrochemically active then $I_{ECL,NP}$ will be 3/5 of $I_{ECL,dye}$; as a consequence, the ECL detection limit is very similar for the free dye and DSNP solutions having the same absorbance.[18] Equation 6 would then allow, by performing two single ECL experiments, evaluating the concentration of $Ru(bpy)_3$ inside DSNPs that effectively contributes to ECL emission ($c_{NP}m$). Accordingly, the ECL emission intensity can then be optimized with respect to DSNP size, doping material, doping level, DSNP charge, ECL coreactant (for example, by varying the size of tertiary amine), supporting electrolyte (the size of ions can influence the rate of penetration of electron into DSNP), electrode material, and solvent.

The present simple model was then tested by comparing the ECL intensity measured at gold SPE electrodes in PB aqueous solutions alternatively of $Ru(bpy)_3^{2+}$ (10^{-5} M) and of DSNP with the same absorbance at the MLCT maximum (Figure S4, Supporting Information) in the presence of TPrA 3×10^{-2} M.

Five different experiments were carried out in each case using a new electrode to check the reproducibility of the ECL signal. Figure 4 shows the typical ECL profile obtained with gold SPE. As expected, one ECL maximum is observed that corresponds to ECL generation principally via mechanism II. The results with basic statistics are summarized in Table 1. From the present investigations we obtain the ECL intensity ratio $R = 0.39$. Since a $c_{NP} = 3.1 \times 10^{-8}$ M can be estimated (see Supporting Information), the value of m (i.e., the number of redox-active centers per DSNP) can be calculated according to eq 8

$$\begin{aligned} \frac{c_{NP}m}{c_{dye}} &= \frac{5}{3} \cdot \frac{I_{ECL,NP}}{I_{ECL,dye}} \Rightarrow m \\ &= \frac{5}{3} \cdot \frac{I_{ECL,NP}}{I_{ECL,dye}} \frac{c_{dye}}{c_{NP}} \\ &= \frac{5}{3} \cdot 0.39 \frac{2 \times 10^{-5}}{3.1 \times 10^{-8}} \\ &\approx 4.2 \times 10^2 \end{aligned} \quad (8)$$

This implies that a remarkable fraction of the $Ru(bpy)_3$ units inside a DSNP, i.e., ca. 65% (=420/650), are electrochemically active, and such an important result is expected to hold even if a more realistic view of DSNPs is assumed in which the presence of nanoporosity, as demonstrated above by the diffusion and reactivity of $TPrA^{\cdot+}$ in DSNPs, is taken into account.

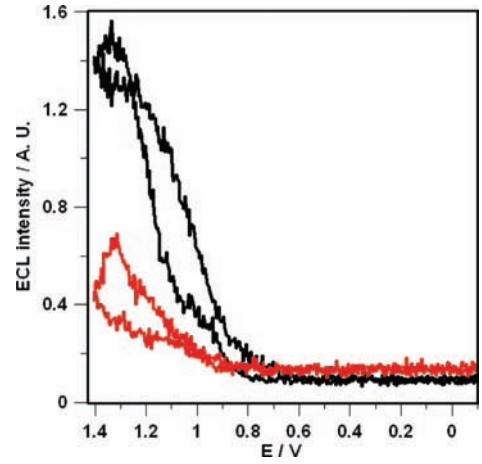

Figure 4. Typical ECL/E profiles of a $Ru(bpy)_3^{2+}$ (black line) and DSNP (red line) solution having the same absorption and [Ru] = 2×10^{-5} M. Potential program: CV, 2 cycles E_0= 0, E_1=1.5 vs Ag, scan rate = 0.2 V/s. Solution: PB 0.1 M/3 $\times 10^{-2}$ M TPrA. Electrode: DROPSENS 220 AT SPE; working electrode material, gold; diameter, 4 mm. Detection: PMT bias 750 V, photocurrent range 10^{-7} A/V. Sample volume: 20 μL/test.

Table 1. Results of ECL Intensity Comparison Tests[a]

test type and no.	max ECL int./au*	comments
$Ru(bpy)_3^{2+}$, 1	1.180	
$Ru(bpy)_3^{2+}$, 2	1.190	$I_{ECL,dye} = 1.184 \pm 0.133$ (11%)
$Ru(bpy)_3^{2+}$, 3	1.060	
$Ru(bpy)_3^{2+}$, 4	1.090	
$Ru(bpy)_3^{2+}$, 5	1.400	
DSNP 1	0.357	
DSNP 2	0.480	$I_{ECL,NP} = 0.462 \pm 0.067$ (15%)
DSNP 3	0.538	
DSNP 4	0.447	
DSNP 5	0.490	$R = 0.39$

[a] Experimental conditions are the same those already described in Figure 4. A new copy of DS220 AT is used in each test. Background signal has been subtracted for maximum ECL intensity.

On the basis of the above result and in view of the higher quantum yields in the case of DSNP with respect to the free $Ru(bpy)_3$ complexes (see above) the ECL generated from a DSNP-SH SAM is therefore expected to be significantly larger than that from a SAM of $Ru(bpy)_3$-SH having the same surface concentrations of redox centers. In fact, in such a case even the only negative effect attributable to NPs, i.e., their slower diffusivity with respect to free complex, would be avoided. Thus, assuming similar m (number of redox-active centers per DSNP) to that estimated in the case of DSNP solution we have

$$\frac{I'_{ECL,NP}}{I'_{ECL,dye}} = fm = 3 \cdot 4.2 \times 10^2 = 1260 \quad (9)$$

where the primed quantities refer to DSNPs and $Ru(bpy)_3^{2+}$ molecules as immobilized species. In fact, a very similar amplification (ca. 500) has been observed comparing the signal obtained from a DSNP-SH SAM with respect to that obtained by the SAM of $Ru(bpy)_3$-SH previously described, although with an expected lower density due to the DSNP diameter.

Concluding Remarks

The DSNP evidenced great chemical and electrochemical stability of the doping and were a suitable platform to introduce

(17) This value of D_{dye} refers to $Ru(bpy)_3^{2+}$ in ethanol solution.
(18) The value of D_{NP} can be modulated by varying the size of DSNP.

the ECL active material in biological buffers. A great ECL signal enhancement (~3 orders of magnitude) was evidenced with respect to single-molecule labels with model systems (DSNP-SH) mimicking probe−target assays. An expected increase of the ECL signal by about 3 orders of magnitude with respect to single molecules can literally open new horizons in the application of DSNPs as labels in probe−target assays such as DNA or proteins detection, and work is now in progress in this direction. Additionally, as demonstrated in the experiments with DSNP-SH, the presence of hydrophobic assembled layers causes further ECL signal increase for the higher amount of $TPrA^{\cdot+}$ electrochemically generated activating the more efficient mechanism I. The higher ECL intensity is in this case a consequence of the quick $TPrA^{\cdot+}$ diffusion rate inside and outside DSNP by reaching redox sites not available for direct and indirect electron hopping (Chart 1). A simple chemical−physical model has been built to quantify experimentally the number of redox centers contributing to ECL per DSNP, allowing optimization of emission performances by varying their physical−chemical properties. In this contribution the potential of the first electrochemical reduction and oxidation of $Ru(bpy)_3^{2+}$ inside DSNP was also estimated for the first time. The values of $E_{1/2,I\ Ox}$ and $E_{1/2,I\ Red}$ were indirectly obtained from the position of the maxima of the ECL emission from cation−anion annihilation. In this context electron transfer between oxidized and reduced $Ru(bpy)_3$ centers appears, surprisingly, to occur between close regions of the same nanoparticle.

The more efficient ECL generation mechanism (mechanism I) involving chemical reduction of $Ru(bpy)_3^{2+}$ to $Ru(bpy)_3^{+}$ by the fast diffusing $TPrA^{\cdot+}$ allows extending the number of emitting redox centers and thickness of ECL active solution with respect to direct and indirect electron hopping (mechanism II). This mechanism, by increasing the amount of generated $TPrA^{\cdot+}$, could be exploited to produce ECL even at relatively long distances from the working electrode as in the surface of cells and tissues in physiological solutions. By this method the restricting need to oxidize directly labeling materials within the relatively short electron tunnelling distance would be avoided, enabling a method analogous to chemiluminescence where reactant is electrochemically generated. Future investigations will be aimed at improvement of DSNP emitting performance by varying size, doping material, doping level, amine size, electrode material, and surface conditioning. Finally, an important property of DSNP to be modulated and optimized is the electrical charge, which is likely to control the number of maximum electrons transferred during electrochemical processes.

Acknowledgment. This work was accomplished in the framework of LATEMAR (www.latemar.polito.it), Centre of Excellence funded by MIUR (Italian Ministry for Education, University and Research) grants (FIRB 2003-2004) for public/private structures involved in research fields characterized by strategic value. The financial support from Fondazione Cassa di Risparmio in Bologna is also gratefully acknowledged. The authors would also like to thank Livio Cognolato, Danilo Bich, and Danilo De Marchi for help in preparing silicon/gold chips.

Supporting Information Available: TEM image of DSNP; DLS profile of DSNP; cyclic voltammetry registered from DSNP-SH-functionalized chips; absorbance spectrum of PB solutions of $Ru(bpy)_3^{2+}$ and DSNP having the same intensity in MLCT maximum; estimation of the DSNP concentration; estimation of the electron-hopping depth in DSNP. This material is available free of charge via the Internet at http://pubs.acs.org.

JA8077158